

Theoretical Predictions and Single-Crystal Neutron Diffraction and Inelastic Neutron Scattering Studies on the Reaction of Dihydrogen with the Dinuclear Dinitrogen Complex of Zirconium

$[P_2N_2]Zr(\mu-\eta^2-N_2)Zr[P_2N_2]$, $P_2N_2 = PhP(CH_2SiMe_2NSiMe_2CH_2)_2PPh$

Harold Basch,^{*,†,‡} Djamaladdin G. Musaev,^{*,†} Keiji Morokuma,^{*,†} Michael D. Fryzuk,^{*,§} Jason B. Love,[§] Wolfram W. Seidel,[§] Alberto Albinati,^{*,⊥} Thomas F. Koetzle,^{*,||} Wim T. Klooster,^{||} Sax A. Mason,^{*,#} and Juergen Eckert^{*,∇}

Contribution from the Cherry L. Emerson Center for Scientific Computation and Department of Chemistry, Emory University, Atlanta, Georgia 30322, Department of Chemistry, University of British Columbia, 2036 Main Mall, Vancouver, British Columbia, Canada V6T 1Z1, Istituto di Chimica Farmaceutica, Università di Milano, I-20131 Milano, Italy, Chemistry Department, Brookhaven National Laboratory, P.O. Box 5000, Upton, New York 11973, Institut Max von Laue - Paul Langevin, 38042 Grenoble Cedex, France, and Los Alamos National Laboratory, Los Alamos, New Mexico 87545

Received July 14, 1998

Abstract: A single-crystal neutron diffraction analysis along with density functional calculations and incoherent inelastic neutron scattering studies has conclusively shown that the dihydrogen adduct of $[P_2N_2]Zr(\mu-\eta^2-N_2)Zr[P_2N_2]$ (**1**) (where $P_2N_2 = PhP(CH_2SiMe_2NSiMe_2CH_2)_2PPh$) is $[P_2N_2]Zr(\mu-\eta^2-N_2H)(\mu-H)Zr[P_2N_2]$ (**2**), the complex with a bridging hydride and a N–N–H moiety, and not the dihydrogen complex $[P_2N_2]Zr(\mu-\eta^2-N_2)(\mu-\eta^2-H_2)Zr[P_2N_2]$ (**3**), as was proposed on the basis of X-ray crystallographic data. In addition, DFT calculations show that the reaction of **1** with both H_2 and SiH_4 is exothermic while an endothermic reaction is found for the reaction of **1** with CH_4 .

The functionalization of molecular nitrogen under mild conditions is still one of the great challenges facing chemists.¹ The industrial success of the Haber–Bosch process, which converts mixtures of N_2 and H_2 to ammonia at high pressures and temperatures in the presence of an activated iron catalyst, has not yet been matched by any other reaction.² Nevertheless, interest in the activation of dinitrogen continues especially from the point of view of its coordination chemistry.^{3–5}

Recently one of us reported⁶ a series of new transformations for a coordinated dinitrogen ligand. It was found that the dinuclear, side-on-bound dinitrogen complex $[P_2N_2]Zr(\mu-\eta^2-N_2)Zr[P_2N_2]$ (**1**) (where $P_2N_2 = PhP(CH_2SiMe_2NSiMe_2CH_2)_2PPh$)

reacts with 1–4 atm of H_2 in toluene solution to form $[P_2N_2]Zr(\mu-\eta^2-N_2H)(\mu-H)Zr[P_2N_2]$ (**2**), containing a N–H bond and a bridging hydride; these conclusions were surmised on the basis of 1H and ^{15}N NMR spectroscopic analysis. However, low-temperature X-ray diffraction studies on crystals isolated from the reaction of **1** with H_2 in hexane did not show the expected NN–H and $Zr(\mu-H)$ features proposed from the solution data, and instead, the diffraction data were interpreted in terms of a complex having a side-on bridging H_2 unit (having a H–H distance of 1.21(5) Å) and an intact side-on N_2 moiety: $[P_2N_2]Zr(\mu-\eta^2-N_2)(\mu-\eta^2-H_2)Zr[P_2N_2]$ (**3**) (Scheme 1). When crystals of **3** were dissolved in d_8 -THF, solution 1H NMR spectroscopy showed the clean formation of **2**. This isomerization process was reported to be reversible, but the mechanism not delineated. A related transformation was also described⁶ for the activation of a Si–H bond of primary silanes $RSiH_3$ to generate the complex $[P_2N_2]Zr(\mu-\eta^2-N_2SiH_2R)(\mu-H)Zr[P_2N_2]$ (**4**; $R = Bu$), the analogue of **2**; in contrast, the solution spectroscopic parameters of **4** matched the molecular structure observed in the solid state. To further probe the mechanism of activation of the H–H and Si–H bonds on **1**, we decided to reinvestigate the experimentally proposed intermediates **2** and **3**, together with the starting N_2 complex, **1**, using quantum chemical methods, neutron diffraction, and incoherent inelastic neutron scattering (INS) spectroscopy. In particular, we obtained single crystals of the proposed intermediate **3** that allowed analysis by neutron diffraction.

Density Functional Calculations

The model complexes chosen in the molecular orbital calculations contain a $[p_2n_2] = (PH_3)_2(NH_2)_2$ unit in place of

[†] Emory University.

[‡] On sabbatical leave from the Department of Chemistry, Bar Ilan University, Ramat Gan, Israel.

[§] University of British Columbia.

[⊥] Università di Milano.

^{||} Brookhaven National Laboratory.

[#] Institut Max von Laue - Paul Langevin.

[∇] Los Alamos National Laboratory.

(1) Gambarotta, S. *J. Organomet. Chem.* **1995**, 500, 117.

(2) Ertl, G. In *Catalytic Ammonia Synthesis*; Jennings, J. R., Ed.; Plenum: New York, 1991.

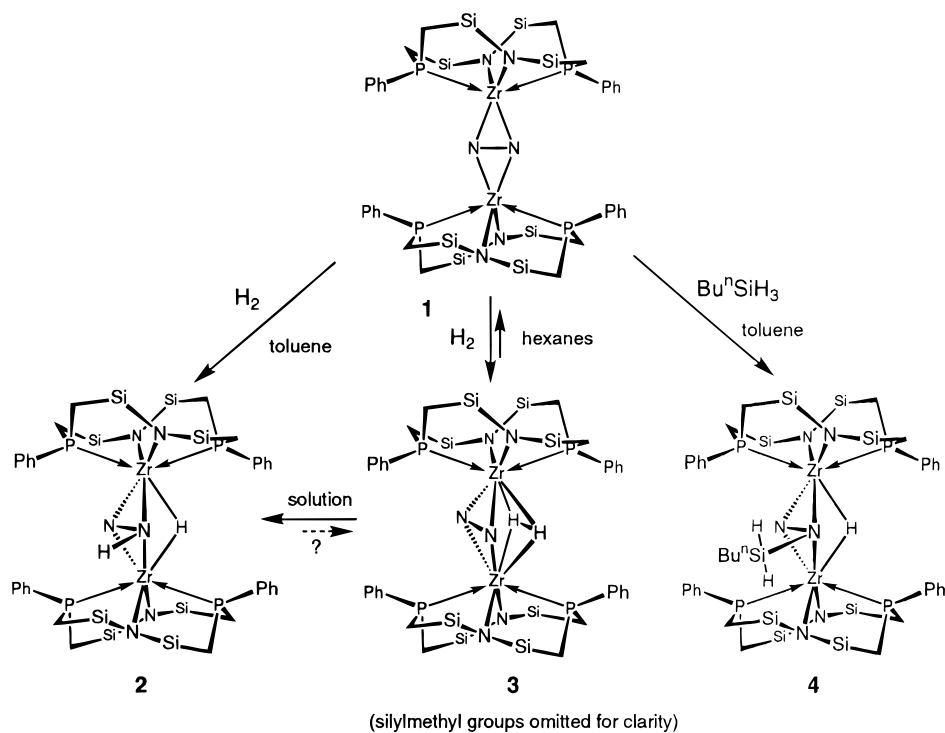
(3) Hidai, M.; Mizobe, Y. *Chem. Rev.* **1995**, 95, 1115.

(4) (a) LaPlaza, C. E.; Cummins, C. C. *Science* **1995**, 268, 861. (b) LaPlaza, C. E.; Johnson, M. J. A.; Peters, J. C.; Odom, A. L.; Kim, E.; Cummins, C. C.; George, G. N.; Pickering, I. J. *J. Am. Chem. Soc.* **1996**, 118, 8623. (c) Odom, A. L.; Arnold, P. L.; Cummins, C. C. *J. Am. Chem. Soc.* **1998**, 120, 5836.

(5) (a) Nishibayashi, Y.; Iwai, S.; Hidai, M. *Science* **1998**, 279, 540. (b) Roussel, P.; Scott, P. *J. Am. Chem. Soc.* **1998**, 120, 1070. (c) O'Donoghue, M. B.; Zanetti, N. C.; Davis, W. M.; Schrock, R. R. *J. Am. Chem. Soc.* **1997**, 119, 2753. (d) Fryzuk, M. D.; Johnson, S. A.; Rettig, S. J. *J. Am. Chem. Soc.* **1998**, 120, 11024.

(6) Fryzuk, M. D.; Love, J. B.; Rettig, S. J.; Young, V. G. *Science* **1997**, 275, 1445.

Scheme 1



the $\text{PhP}(\text{CH}_2\text{SiMe}_2\text{NSiMe}_2\text{CH}_2)_2\text{PPh}$ used experimentally.⁶ In other words, the coordinated phosphines and nitrogens of the tetradentate macrocyclic $[\text{P}_2\text{N}_2]$ on each Zr atom are preserved, while H atoms replace two CH_2 groups and a phenyl on each phosphorus and two SiMe_2 groups on each nitrogen. As two NH_2 groups account for two electrons and the bridging N_2 molecule accounts for two more per zirconium,⁶ each Zr is formally d^0 and the electronic ground state of the complex is a closed-shell singlet.

The density functional method B3LYP⁷ studies of the model compounds, $[\text{p}_2\text{n}_2]\text{Zr}(\mu\text{-}\eta^2\text{-N}_2)\text{Zr}[\text{p}_2\text{n}_2]$ (**1m**), $[\text{p}_2\text{n}_2]\text{Zr}(\mu\text{-}\eta^2\text{-N}_2\text{H})(\mu\text{-H})\text{Zr}[\text{p}_2\text{n}_2]$ (**2m**), $[\text{p}_2\text{n}_2]\text{Zr}(\mu\text{-}\eta^2\text{-N}_2\text{CH}_3)(\mu\text{-H})\text{Zr}[\text{p}_2\text{n}_2]$, (**2'm**), $[\text{p}_2\text{n}_2]\text{Zr}(\mu\text{-}\eta^2\text{-N}_2\text{SiH}_2\text{R})(\mu\text{-H})\text{Zr}[\text{p}_2\text{n}_2]$ (**4m**), and $[\text{p}_2\text{n}_2]\text{Zr}(\mu\text{-}\eta^2\text{-N}_2)(\mu\text{-}\eta^2\text{-H}_2)\text{Zr}[\text{p}_2\text{n}_2]$ (**3m**), have been performed using the Stevens–Basch–Krauss (SBK)⁸ effective core potentials (ECP) (it is a relativistic ECP for the Zr atoms) with the standard 4-31G, CEP-31, and (8s8p6d/4s4p3d) basis sets for the H, C, and P; N; and Zr atoms, respectively. Our calculations⁹ have shown that the addition of the polarization d function is important for the N atoms ($\alpha_d = 0.8$) of the bridging N_2 unit, but is not important for the N and P atoms of the external $[\text{p}_2\text{n}_2]$ groups.

The calculated geometries of all the intermediates are shown in Figure 1, along with their relative energies. The model dinitrogen complex, **1m**, is calculated to have approximately C_2 symmetry and a bent $\text{Zr-N}_2\text{-Zr}$ unit,¹⁰ while **1** is experimentally found to have a coplanar $\text{Zr-N}_2\text{-Zr}$.⁶ The structure

of **1m** with a coplanar $\text{Zr-N}_2\text{-Zr}$ unit (in D_{2h} symmetry) is calculated to be 24.4 kcal/mol less stable. The origin of the bend is probably electronic in nature, i.e., due to more extensive opportunities for orbital mixing between the Zr (4d, 5s, and 5p) and molecular nitrogen (σ , σ^* , π , π^*) valence orbitals in the lower symmetry. The ancillary macrocyclic ligand structure could likely prevent the bending in the real complex **1**, and indeed other ancillary ligands do support bent, side-on bridging N_2 units.¹⁰

We used D_{2h} symmetry with a coplanar $\text{Zr-N}_2\text{-Zr}$ unit and examined the different possible arrangements of the NH_2 and PH_3 ligands relative to the bridging N-N axis. One has the N-N axis of the two NH_2 ligands attached to each Zr atom oriented *perpendicular* ($\varphi = 90^\circ$) to the N-N axis of the bridging N_2 molecule. Another has these axes *parallel* ($\varphi = 0^\circ$) to each other, so that the P-P axis of the two PH_3 ligands on each Zr atom is perpendicular to the bridging N-N axis. The former structure is calculated to be more stable than the latter by 18 kcal/mol. This result can be understood in terms of the larger repulsion in the latter between the negatively charged nitrogen atoms in NH_2 ($-0.83e$) and the bridging N_2 atoms ($-0.45e$). An attempt to optimize starting with $\varphi = 45^\circ$ converged to the structure **1m**; this structure (Figure 1) is the most stable isomer of the reactant complex with regard to the arrangement of the NH_2 and PH_3 groups, in accord with experiment.⁶ Comparison of the calculated **1m** (bent) and the experimental⁶ **1** geometries shows some discrepancies in the bond lengths of up to 0.1 Å, which could be a result of the simplified $[\text{p}_2\text{n}_2]$ model used; this is under further investigation.⁹

As mentioned above, the experimentally indicated products of the reaction of **1** with H_2 and primary silanes are complexes **2** and **4**, respectively.⁶ We have found complex **2** for the $\text{HX} = \text{H}_2$ (**2m**), CH_4 (**2'm**), and SiH_4 (**4m**). One feature of these model complexes is the asymmetry calculated for the bridging $\text{Zr}^1\text{-H}^2\text{-Zr}^2$ unit. As seen from Figure 1, the $\text{Zr}^1\text{-H}^2$ distance is always 5–10% shorter than $\text{Zr}^2\text{-H}^2$. Although such differences would be difficult to detect via X-ray crystallography or

(7) (a) Becke, A. D. *Phys. Rev. A* **1988**, *38*, 3098. (b) Lee, C.; Yang, W.; Parr, R. G. *Phys. Rev. B* **1988**, *37*, 785. (c) Becke, A. D. *J. Chem. Phys.* **1993**, *98*, 5648. (d) Stephens, P. J.; Devlin, F. J.; Frisch, M. J.; Chabalowski, C. F. *J. Phys. Chem.* **1994**, *98*, 11623.

(8) (a) Stevens, W. J.; Basch, H.; Krauss, M. *J. Chem. Phys.* **1984**, *81*, 6026. (b) Stevens, W. J.; Krauss, M.; Basch, H.; Jasien, P. G. *Can. J. Chem.* **1992**, *70*, 612.

(9) Basch, H.; Musaev, D. G.; Morokuma, K. To be submitted for publication.

(10) (a) Cohen, J. D.; Fryzuk, M. D.; Loehr, T. M.; Mylvaganam, M.; Rettig, S. J. *Inorg. Chem.* **1998**, *37*, 112. (b) Duchateau, R.; Gambarotta, S.; Beydoun, N.; Bensimon, C. *J. Am. Chem. Soc.* **1991**, *113*, 8986.

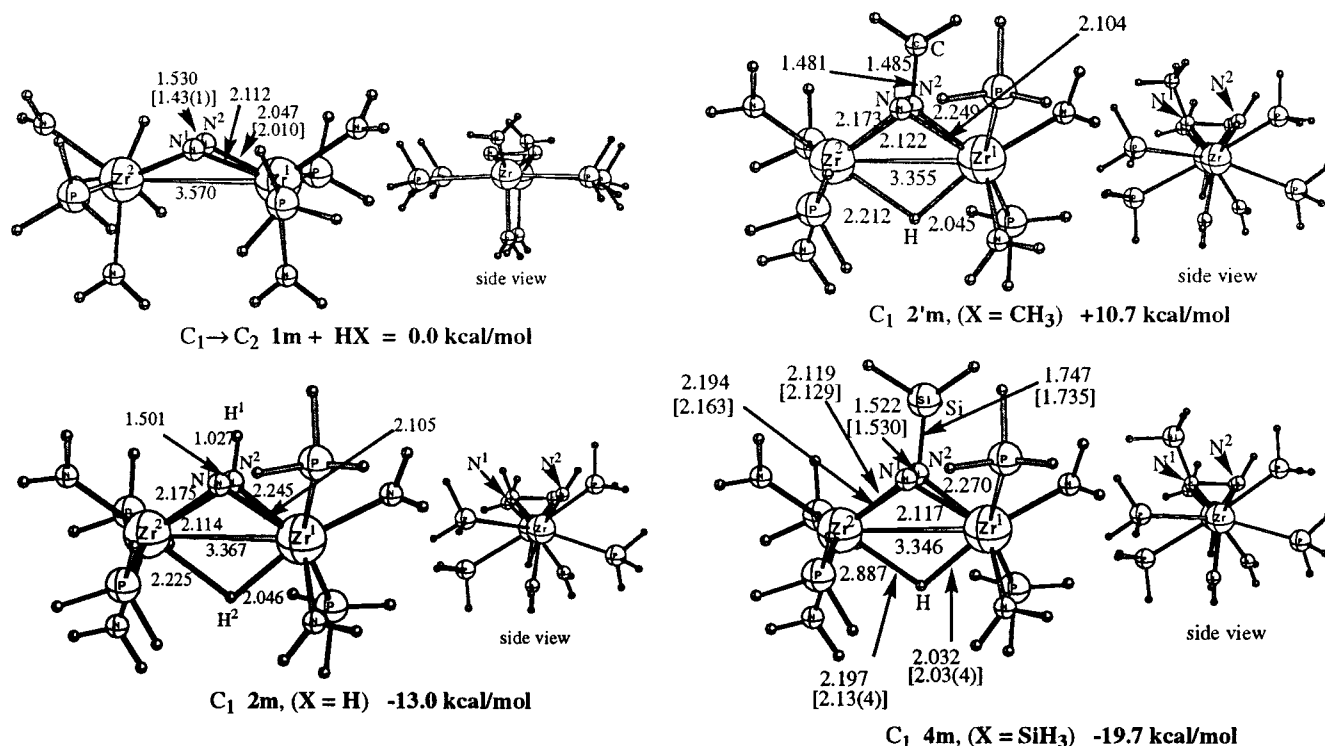


Figure 1. Calculated geometries (distances in angstroms) and energies (kcal/mol, relative to the corresponding reactants) of the reactant, **1m**, and complexes, **2m**, **2'm**, and **4m**, corresponding to the X = H, CH₃, and SiH₃, respectively. In brackets are the experimental results for **1**.

neutron diffraction, the overall geometry of the complex **4m** presented in Figure 1 is in good agreement with X-ray results for **4**.⁶ One should note that the change in X via H to CH₃ to SiH₃ only slightly reduces the Zr¹–H and Zr²–H bond distances. Meanwhile, the calculated N¹–N² bond distance changes from 1.501 Å (X = H) to 1.485 Å (X = CH₃) to 1.522 Å (X = SiH₃). The overall reaction **1m** (bent) + HX → **2m**, **2'm**, or **4m** is calculated to be exothermic by 13.0 kcal/mol for X = H, endothermic by 10.7 kcal/mol for X = CH₃, and again exothermic by 19.7 kcal/mol for X = SiH₃. This trend in the energetics is expected as follows. During this reaction the H–X bond is broken, and N–X and Zr¹–H–Zr² bonds are formed. In accord with the above discussion of the geometry of the Zr¹–H–Zr² units, the Zr¹–H–Zr² binding energy can be roughly taken as constant upon changing X. Therefore, the calculated trend in the energetics of the reaction, **1** + HX → **2** will reflect the energy difference between the broken H–X and formed N–X binding energies. If we use experimental values of the H–X (104.2, 104.7, and 90.3 kcal/mol for X = H, CH₃, and SiH₃, respectively) and N–X (107.4, 84.7, and 100.1 kcal/mol for H₂N–X, where X = H, CH₃, and SiH₃, respectively) binding energies,¹¹ we obtain –3.2, +20.0, and –9.8 kcal/mol for X = H, CH₃, and SiH₃, respectively, the same trend as that found above for the present reaction.

Conspicuously absent from the calculated results in Figure 1 is structure **3**, the dihydrogen complex proposed from X-ray studies. Repeated computational efforts starting from different initial guesses all led to dissociation of the H₂ molecule or to **2m**. The use of a larger basis set, ([5s1p]/[3s1p]), on the molecular hydrogen atoms did not change this result.

Neutron Diffraction and INS Studies

Given that structure **3** was not detected in solution and the intrinsic difficulties in locating hydrogens by X-ray crystal-

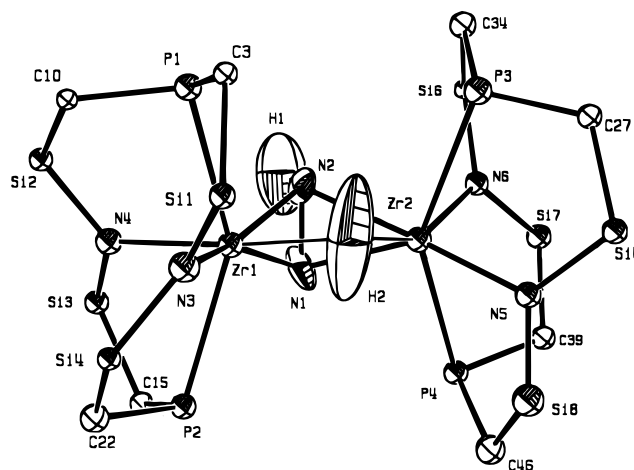


Figure 2. ORTEP view of $[P_2N_2]Zr(\mu-\eta^2-N_2H)(\mu-H)Zr[P_2N_2]$ (**2**) showing the inner core and the positions of the hydrogen atoms. The silyl methyl groups and phosphorus phenyl substituents have been omitted for the sake of clarity.

lography, we used neutron diffraction to definitively locate the hydrogen atoms in this structure. Suitable orange crystals deposited after 3 weeks from a toluene/hexanes solution of dinitrogen complex **1** under 4 atm of H₂. The neutron diffraction study was performed at 25 K, and the results are shown in Figure 2; the crystal data (unit cell and space group) match those of the original report.⁶ What immediately becomes apparent is that the solid-state structure is not the dihydrogen adduct **3** proposed from the low-temperature X-ray data, but rather **2**, the complex proposed from the solution data.⁶ The hydride is located symmetrically bridging the two zirconium centers with Zr–H bond distances of 1.95(6) and 1.98(6) Å, while the hydrogen attached to the N₂ moiety has a N–H bond length of 0.93(6) Å. The atomic displacement parameters for the bridging hydride are sufficiently large even at 25 K to account for the incorrect assumption that this was due to two hydrogen atoms side-on-

(11) CRC Handbook of Chemistry and Physics, 72nd ed.; Lide, D. R., Ed.; CRC Press: Boca Raton–Ann Arbor–Boston, 1992.

Table 1. Selected Bond Lengths (Å) and Angles (deg) from Neutron and X-ray Diffraction for $\{[P_2N_2]Zr\}_2(\mu-H)(\mu-\eta^2-N_2H)$, **2**^a

	neutron	X-ray ^b	DFT calculations ^c
Zr1–Zr2	3.25(1)	3.2723(4)	3.367
Zr1–H1	2.73(6)		
Zr1–H2	1.95(6)		2.046
Zr2–H2	1.98(6)		2.225
Zr1–N1	2.09(2)	2.120(3)	2.105
Zr1–N2	2.11(2)	2.125(3)	2.245
Zr1–N3	2.26(1)	2.254(3)	2.119
Zr1–N4	2.21(1)	2.199(3)	2.128
Zr1–P1	2.71(2)	2.719(1)	2.900
Zr1–P2	2.74(1)	2.755(1)	3.036
Zr2–N1	2.09(1)	2.125(3)	2.114
Zr2–N2	2.15(2)	2.160(3)	2.175
Zr2–N5	2.21(1)	2.232(3)	2.140
Zr2–N6	2.18(2)	2.207(3)	2.107
Zr2–P3	2.74(2)	2.761(1)	2.946
Zr2–P4	2.76(2)	2.738(1)	2.888
N1–N2	1.39(2)	1.443(5)	1.501
N2–H1	0.93(6)		1.027
Zr1–H2–Zr2	112. (2)		
Zr1–N1–Zr2	102.0 (6)	102.0(1)	
Zr1–N2–Zr2	99.1(7)	99.6(1)	
H2–Zr2–N1	72. (2)		
H2–Zr1–N1	73. (2)		
P1–Zr1–N1	126.6(6)	126.3(1)	
P1–Zr1–N2	88.1 (6)	86.77(9)	
P1–Zr1–H2	95. (2)		
P1–Zr1–N3	73.8(5)	74.07(7)	
P1–Zr1–N4	85.4(5)	84.83(8)	
N3–Zr1–N1	154.2(7)	153.5(1)	
N4–Zr1–H2	170. (2)		
P3–Zr2–N1	127.7(6)	127.6(1)	
P3–Zr2–N2	90.0 (6)	88.3(1)	
P3–Zr2–H2	82. (2)		
P3–Zr2–N5	84.2(6)	84.57(8)	
P3–Zr2–N6	75.7(5)	75.80(8)	
N5–Zr2–N2	159.1(6)	158.6(1)	
N6–Zr2–H2	153. (2)		

^a Also included are the calculated bond lengths from DFT. Estimated standard deviations are given in parentheses. ^b X-ray values are taken from ref 6. ^c DFT values are taken from this work. See Figure 1.

bound with a H–H distance of 1.21 Å. The large displacement shows that the hydride sits in an extremely soft potential, for motion perpendicular to the Zr–Zr vector. This is compatible with the low-lying bending mode observed in the INS spectrum (vide infra), which further confirms the presence of the bridging hydride ligand. Other bond lengths and bond angles from the neutron study are given in Table 1 with comparison to the data obtained from the DFT calculations and the X-ray crystal structure.⁶

Confirmation of the above result was obtained by an INS study. Neutron spectroscopy has the major advantage over conventional spectroscopic techniques (i.e., IR and Raman) in that INS spectra are dominated¹² by the modes involving hydrogen atoms due to the following: (i) the neutron incoherent scattering cross-section¹³ of hydrogen is much larger than that of any other atom and (ii) the INS band intensities are also enhanced by the large-amplitude motions of the H atoms. This technique has therefore been very successful¹⁴ in identifying vibrations of both hydride and dihydrogen ligands present in large complex molecules.

Frequencies of the main peaks from the difference INS spectrum [$\{[P_2N_2]Zr\}_2(\mu-H)(\mu-\eta^2-N_2H) - \{[P_2N_2]Zr\}_2(\mu-\eta^2-N_2)$] (see the Experimental Section) appear in Table 2. For the purpose of this discussion we will describe the modes for the ($\mu-H$) and ($\mu-\eta^2-N_2H$) ligands separately. A complete vibrational

Table 2. Vibrational Frequencies (cm⁻¹)^a and Approximate Descriptions of the Modes for $\{[P_2N_2]Zr\}_2(\mu-H)(\mu-\eta^2-N_2H)$, **2**, Obtained by the Spectral Difference Technique (See the Text)

assignment	obsd frequency	assignment	obsd frequency
$\delta(ZrHZr)$ (OP)	190	$\delta(Zr(NNH)Zr)$	670 (v br)
not assigned ^b	235	$\delta(NNH)$	906
$\delta(Zr(NNH)Zr)$	288	$\nu_s(ZrHZr)$	1053
$\delta(ZrHZr)$ (IP)	356	$\nu_{as}(ZrHZr)$	1359
$\delta(Zr(NNH)Zr)$	455		

^a Uncertainties in the frequencies are approximately 2% of their value. ^b See the text.

analysis of these modes with at least the skeleton of the remainder of the complex would, of course, be preferable but is beyond the scope of this paper.

The vibrational modes of bridging hydrides are well-known¹⁵ and consist of a symmetric and an antisymmetric M–H–M stretching mode, as well as in-plane and out-of-plane deformations of the LM–H–ML unit.

On the basis of the Zr–H–Zr angle $\theta = 112^\circ$ determined by neutron diffraction, and the modified correlation of ν_{as}/ν_s vs $\tan(\theta/2)$ reported by some of us,¹⁶ we can readily assign the peaks at 1053 and 1359 cm⁻¹ to ν_s and ν_{as} , respectively.

While the deformation modes are usually found¹⁶ in the range of 300–700 cm⁻¹, the strongest peak in our INS at 190 cm⁻¹ must be assigned to the out-of-plane deformation (OP) in view of the very large rms displacement (approximately 0.69 Å) calculated from the anisotropic displacement parameter for the bridging hydride in a direction perpendicular to the Zr–H–Zr plane. This large amplitude suggests an unusually “soft” vibrational frequency and is therefore in good agreement with the strong INS band at 190 cm⁻¹. The in-plane deformation mode (IP), on the other hand, may be assigned to the band at 356 cm⁻¹.

A peak observed at 235 cm⁻¹ is more difficult to assign. It gains INS intensity in going to $\{[P_2N_2]Zr\}_2(\mu-H)(\mu-\eta^2-N_2H)$ from $\{[P_2N_2]Zr\}_2(\mu-\eta^2-N_2)$, which implies that this mode involves a deformation of the $[P_2N_2]Zr(\mu\text{-bridge})Zr[P_2N_2]$ skeleton.

The modes of the bridging ($\mu-\eta^2-N_2H$) moiety can only be crudely discussed without a full vibrational analysis. N₂H itself will have three modes: $\nu(NN)$, $\nu(NH)$, and the deformation mode $\delta(NNH)$. The latter is the only one of these modes that should have observable INS intensity, and it can thus readily be assigned at 906 cm⁻¹, a frequency that corresponds roughly to the average of the symmetric and antisymmetric NH₂ wags in hydrazine.¹⁷ One would also expect to observe approximate deformation modes (twist, wag, and rock) of the entire ($\mu-\eta^2-N_2H$) ligand relative to the rest of the complex, i.e., LZr–ZrL. We tentatively assign the bands at 288, 455, and 670 cm⁻¹ to these modes (not necessarily in this order).

Conclusions

The neutron studies and the DFT results agree with one another and show conclusively that the dinuclear dihydrogen

(12) Archer, J.; Lehmann, M. S. *J. Appl. Crystallogr.* **1986**, *19*, 456.

(13) Koester, L.; Rauch, M.; Herkens, M.; Schröder, K. K. F. A. *Report Jül – 755*; K. F. A. Jülich: Germany, 1981.

(14) Eckert, J. *Trans. Am. Cryst. Assoc.* **1995**, *31*, 45.

(15) Braid, I. J.; Howard, J.; Tomkinson, J. J. *Chem. Soc., Faraday Trans. 2*, **1983**, *79*, 253.

(16) Taylor, A. D.; Wood, E. J.; Goldstone, J. A.; Eckert, J. J. *Nucl. Instrum. Methods Phys. Res.* **1984**, *221*, 408.

(17) Tipton, T.; Stone, D. A.; KuBulat, K.; Person, W. B. *J. Phys. Chem.* **1989**, *93*, 2917.

Table 3. Crystallographic and Experimental Data for the Neutron Diffraction Study of $\{[P_2N_2]Zr\}_2(\mu-H)(\mu-\eta^2-N_2H)$, **2**

formula	$C_{48}H_{86}N_6P_4Si_8Zr_2$
fw	1278.27
crystal dimensions, mm	$0.5 \times 1.3 \times 2.1$
crystal system	orthorhombic
space group	$P2_12_12_1$
data colln, T (K)	25(1)
a, Å	12.149(3)
b, Å	20.856(5)
c, Å	24.515(7)
V, Å ³	6212(1)
Z	4
D_{calcd} , g cm ⁻³	1.366
wavelength λ , Å	1.5377(3) (Cu(200) monochromated)
absorption coeff μ , cm ⁻¹	2.81
transmission coeffs	0.8618–0.6728
no. of reflections	8073
no. of indep reflections (n_o)	2629
no. of params refined (n_v)	637
R_{av}	0.075
R_{w2}^a (all data)	0.169
R^a	0.135
GOF ^a	3.62

$$^a R_{w2} = [\sum w(F_o^2 - F_c^2)^2 / \sum w(F_o^2)^2]^{1/2}; R = [\sum |(F_o^2 - F_c^2)| / \sum (F_o^2)];$$

$$\text{GOF} = [\sum w(F_o^2 - F_c^2)^2 / (n_o - n_v)]^{1/2}.$$

complex **3** proposed earlier does not exist, but rather is an artifact of the X-ray analysis. Instead, the solution structure **2** proposed on the basis of NMR spectral analysis is in fact identical to the solid-state structure. The observation that the dinitrogen complex **1** can activate H₂ and silanes to form N–H and N–Si bonds, respectively, is significant since these are new transformations for a coordinated dinitrogen moiety.

Experimental Section

DFT Calculations. Details are given in the text.

Neutron Diffraction Study of $\{[P_2N_2]Zr\}_2(\mu-H)(\mu-\eta^2-N_2H)$, **2.** An orange, transparent, prismatic crystal of the title compound, of volume ~ 1.4 mm³, obtained by slow crystallization from a toluene/hexanes (4:1) solution of $\{[P_2N_2]Zr\}_2(\mu-\eta^2-N_2)^6$ under H₂, was glued with a two-component glue (Kwikfill) on an Al pin under a hydrogen atmosphere and then sealed in a quartz cap to prevent H₂ loss. The sample was transferred to a DISPLEX cryorefrigerator¹² on the thermal-beam instrument D19 at the ILL reactor, equipped with a $4^\circ \times 64^\circ$ position-sensitive detector.¹⁸ A Cu(200) monochromator in reflection (nominal takeoff angle 75°) was used to select a neutron beam of wavelength 1.5377(3) Å.

The sample was slowly cooled (1 °C/min) to 25 K, while a strong reflection was monitored. No change in mosaic or splitting of the peak was observed. The room-temperature space group $P2_12_12_1$ was confirmed at 25 K. The final cell constants were obtained, at the end of the data collection, by a least-squares fit to the centroids of 2042 well-behaved strong reflections. Further experimental details are summarized in Table 3.

Intensity data ($+h$, $\pm k$, $+l$), up to $2\theta \leq 40^\circ$, were measured by means of ω scans, in equatorial geometry, while higher angle data were recorded in normal beam geometry. Because of the rather weak diffraction by the crystal, a long measuring time, about 19 s per step in ω , was required for adequate counting statistics at higher 2θ values, so measurements with $2\theta > 90^\circ$ were not attempted. Two standard reflections were monitored regularly and showed no significant variation.

Bragg intensities were integrated in 3-D using the ILL program Retreat.¹⁹ In all, 8073 reflections were recorded, 1720 of which were

(18) Thomas, M.; Stansfield, R. F. D.; Berneron, M.; Filhol, A.; Greenwood, G.; Jacobe, J.; Feltn, D.; Mason, S. A. In *Position-Sensitive Detection of Thermal Neutrons*; Convert, P., Forsyth, J. B., Eds.; Academic Press: London, 1983; p 344.

rejected because of possible interference by peaks from preferred orientation in the Al sample pin. The remaining 6353 intensities were corrected analytically for absorption by using the program D19abs (based on the ILL version of the CCSL system²⁰). This was followed by a Lorentz correction and averaging to yield squared structure factors, F_o^2 , for 2629 independent reflections.

The initial atomic coordinates for the heavy atoms were taken from the X-ray structural determination.⁶ Full-matrix, least-squares refinements were performed with the program UPALS,²¹ minimizing the function $\sum w(F_o^2 - (k^2F_c^2))^2$, with weights $w = [\sigma^2(F_o^2) + (0.02F^2)^2]^{-1}$ and using all the independent data including those with negative intensities. Neutron scattering lengths (fm) were taken to be $b_{Zr} = 7.160$, $b_{Si} = 4.149$, $b_P = 5.130$, $b_C = 6.646$, $b_N = 9.360$, and $b_H = -3.741$.¹³

As expected from the small size of the crystal the observed scattering was weak, and therefore the quality of the data set allowed only a limited number of parameters to be refined, producing a structural determination of limited precision.

During the refinement the difference Fourier maps clearly revealed all of the H atom positions of the $[P_2N_2]$ ligand and showed only one negative peak between the two Zr atoms, corresponding to a bridging hydrido ligand, and a second negative peak at ~ 1 Å from N1, thus revealing the presence of an “NN–H” ligand.

The final structure model included coordinates and isotropic displacement parameters for all atoms, except for the bridging hydride and the atoms of the “NNH” moiety which were treated anisotropically. No extinction correction was deemed necessary. The refinement was terminated when $\Delta p/\sigma(p)$ for all parameters was ≤ 0.02 . A difference Fourier synthesis, computed at this point, showed no significant features. Final atomic coordinates with equivalent isotropic displacement parameters and anisotropic displacement parameters are given in Table S1 and S2 in the Supporting Information.

On warming the crystal to room temperature, it was still orange exactly as before the experiment. However, after 4 days at room temperature, the crystal had become white/transparent presumably because the epoxy seal between the quartz cap and the Al pin was no longer airtight, so that hydrogen was lost from the sample. The white crystal (though still of crystalline appearance, without surface powder) appeared not to diffract.

Incoherent Inelastic Neutron Scattering (INS) Study of $\{[P_2N_2]Zr\}_2(\mu-H)(\mu-\eta^2-N_2H)$, **2.** The INS spectra were obtained at 15 K, on the FDS instrument²² at the Manuel Lujan Jr. Neutron Scattering Center of Los Alamos National Laboratory. The time-of-flight FDS spectrometer covers the energy range 250–4000 cm⁻¹ with a resolution of 2–10% of the incident neutron energy.

Approximately 1–2 g samples, sealed under helium atmosphere in aluminum sample holders, were used for these experiments. A spectral difference technique¹⁶ was utilized to highlight the vibrational modes of the H atoms in the (μ -H) and (μ - η^2 -NNH) moieties by subtraction of the INS spectrum of the dinitrogen compound $\{[P_2N_2]Zr\}_2(\mu-\eta^2-N_2)$ from that of $\{[P_2N_2]Zr\}_2(\mu-H)(\mu-\eta^2-N_2H)$. This technique serves to eliminate from the difference spectrum the bands arising from the vibrational modes involving the hydrogen atoms of the $[P_2N_2]$, provided that their motions are not coupled to those from the (μ -H) and (μ - η^2 -NNH) groups or the coupling is negligible. However, this technique requires a spectrometer with very high counting rates to obtain reasonable statistical precision on the difference data set. The FDS spectrometer is particularly well suited for this type of experiment.²³

Acknowledgment. H.B. acknowledges a Visiting Fellowship from the Emerson Center. The present research is in part supported by a grant (CHE-9627775) from the National Science

(19) Wilkinson, C.; Khamis, H. W.; Stansfield, R. F. D.; McIntyre, G. J. *J. Appl. Crystallogr.* **1988**, *21*, 471.

(20) Matthewman, J. C.; Thompson, P.; Brown, P. J. *J. Appl. Crystallogr.* **1982**, *15*, 167.

(21) Lundgren, J. O. *Crystallographic Computer Programs*; Report UUC-B13-4-05; Institute of Chemistry, University of Uppsala: Uppsala, Sweden, 1982.

(22) Eckert, J. *Physica* **1986**, *136B*, 150.

(23) Albinati, A.; Chaloupka, S.; Eckert, J.; Venanzi, L. M.; Wolfer, M. K. *Inorg. Chim. Acta* **1997**, *259*, 305.

Foundation (K.M.), by NSERC of Canada (M.D.F.), and by the Alexander von Humboldt Foundation (Feodor Lynen Fellowship to W.W.S.). Work at Brookhaven National Laboratory was performed under Contract DE-AC02-98CH10886 with the U.S. Department of Energy, Office of Basic Energy Sciences. The neutron diffraction measurements were carried out at the Institut Max von Laue - Paul Langevin, Grenoble, and the inelastic neutron scattering spectrum was recorded at the Manuel Lujan Jr. Neutron Scattering Center of Los Alamos National Laboratory.

Supporting Information Available: The x , y , and z coordinates for structures **1m**, **2m**, **2'm**, and **4m** calculated from the DFT calculations, additional tables of positional parameters, atomic displacement parameters, the extended list of the bond lengths and bond angles for **2** from the neutron diffraction study, and a fully labeled ORTEP diagram (21 pages, print/PDF). See any current masthead page for ordering information and Web access instructions.

JA9824831